Title	Electrodeposited poly(3,4-ethylenedioxypyrrole) films as neural interfaces: Cytocompatibility and electrochemical studies
Author(s)	Krukiewicz, Katarzyna; Kowalik, Agnieszka; Czerwinska-Glowka, Dominika; Biggs, Manus J. P.
Publication Date	2019-02-06
Publication Information	Krukiewicz, Katarzyna, Kowalik, Agnieszka, Czerwinska-Glowka, Dominika, & Biggs, Manus J. P. (2019). Electrodeposited poly(3,4-ethylenedioxypyrrole) films as neural interfaces: Cytocompatibility and electrochemical studies. Electrochimica Acta, 302, 21-30. doi:10.1016/j.electacta.2019.02.023
Publisher	Elsevier
Link to publisher's version	https://doi.org/10.1016/j.electacta.2019.02.023
Item record	http://hdl.handle.net/10379/15019
DOI	http://dx.doi.org/10.1016/j.electacta.2019.02.023

Electrodeposited poly(3,4-ethylenedioxypyrrole) films as neural interfaces: cytocompatibility and electrochemical studies

Katarzyna Krukiewicz[1,2,*], Agnieszka Kowalik[2], Dominika Czerwińska-Główka[2], Manus J.P. Biggs[1]

[1]Centre for Research in Medical Devices, National University of Ireland, Galway, Ireland

[2]Department of Chemistry, Silesian University of Technology, Gliwice, Poland

*Corresponding author:

Katarzyna Krukiewicz, PhD

Katarzyna.krukiewicz@nuigalway.ie

ISE member

Declarations of interest:
none

Abstract

Conducting polymers have been extensively reported as promising coating materials for applications involving interactions with electrically excitable tissues. Specifically, metal electrodes functionalized with conducting polymer coatings have been employed as biointerface presenting tailored properties to promote electrode integration as well as chronic functionality. Currently, polypyrrole (PPy) and poly(3,4-ethylenedioxythiophene) (PEDOT) represent the most extensively studied conducting polymers, exhibiting favourable electrochemical properties and biocompatibility. In this paper, we study electrodeposited poly(3,4-ethylenedioxypyrrole) (PEDOP), a conducting polymer which is structurally related to both PEDOT and PPy, and is expected to outperform its "parent" polymers in terms of electrochemical properties and biocompatibility. The performance of PEDOP doped with chloride/phosphate, *p*-toluenesulfonate or polystyrene sulfonate was subsequently investigated to assess the efficacy of these ionic dopants in promoting electrochemical stability and neural cytocompatibility. Electrodeposited PEDOP films exhibited a high charge storage capacity (50.07 ± 6.96 mC cm^{-2}), charge injection capacity (203 ± 24 μC cm^{-2}) and substantial stability (performance loss of 0.49 ± 0.06 % after 100 000 stimulation pulses). Furthermore, PEDOP films promoted enhanced neuron outgrowth and viability relative to control substrates. In particular, PEDOP/PTS was shown to increase the average neurite length three times when compared with cells cultured on bare Pt control. Consequently, due to its favourable electrochemical characteristics together with high neural cytocompatibility, PEDOP can be indicated as a promising alternative to PPy and PEDOT in the field of neural science.

Keywords

conducting polymers; cytocompatibility; neural interface; poly(3,4-ethylenedioxypyrrole)

1. Introduction

Conducting polymers have been used for biomedical engineering purposes for the last 25 years [1,2], due to their unique ability to combine the electrical properties of metallic materials and chemomechanical properties of polymers [3]. In particular, conducting polymers are organic, soft and wet materials promoting ionic transfer, and enhanced biomimicry [4], while presenting semi-conductor characteristics, with a conductivity range of 100-200 S/cm [5]. Various conducting polymers and their composites have been described as promising materials for applications involving interactions with electrically excitable tissues [6]. In particular, conducting polymer coatings have been shown to address the challenges associated with peri-implant gliosis, fibrous encapsulation which significantly reduces chronic functionality of neural electrodes *in vivo* [6]. Consequently, metal electrodes functionalized with conducting polymer coatings have been found to provide a biointerface with tailorable properties that promote electrode integration as well as chronic functionality [7,8].

Due to the low oxidation potential, water-solubility and commercial availability of pyrrole [9], pyrrole-derived polymers were the first extensively studied conducting polymers with biological applications [10]. Polypyrrole (PPy) has been studied for the design of artificial muscles [11], drug delivery system [12] and neuronal scaffolds [13]. Recently, however, research into PPy in biomedical engineering has been surpassed by poly(3,4-ethylenedioxythiophene) (PEDOT) [14], due to its higher electrical conductivity and stability [15]. Despite all its benefits, the performance of PEDOT is limited by the low water solubility of its monomer, EDOT, narrowing the application of this polymer as a biomaterial. It follows that an ideal material for tissue engineering applications should possess the favorable water solubility and low oxidation potential of pyrrole, together with high stability of PEDOT. Structurally related to both PEDOT and PPy, poly(3,4-ethylenedioxypyrrole) (PEDOP) exhibits a combination of the qualities of its “parent” polymers, resulting in the formation of a

superior conducting material [16,17]. Recently, PEDOP has been successfully used in the development of sensors [18], biosensors [19] and drug carriers [20]. The major restraint of applying PEDOP *in vivo* is the lack of the cell studies verifying its biocompatibility. Therefore, PEDOP has been known as a versatile but underutilized electroactive and conducting polymer, especially in the field of bioengineering [21]. Although it can be inferred that PEDOP may perform well in neural interfacing applications [21], the neural cytocompatibilty of thin-film PEDOP coatings has yet to be resolved.

The performance of conducting polymers is dependent on the doping ion that is introduced into the structure of polymer chain during the polymerization process [22]. The doping ion is used to maintain the electroneutrality of the polymer, since the process of polymerization involves the formation of radical cations [23]. Through the choice of dopant, it is possible to tailor such properties as electrical conductivity [24], surface morphology [25] and polymer elasticity [26], considerations for the design of a neural interface technologies. The most well studied dopants for oxidative polymerization include buffer salts and perchlorates, and more recently, aromatic sulfonate compounds, such as *p*-toluenesulfonate (PTS) and polystyrene sulfonate (PSS) [5]. These dopants are known for providing conducting polymers with numerous beneficial properties, including their significant biocompatibility and processability [7,27].

In this study, the effects of electrodeposited PEDOP on the electrochemical and cytocompatibility performance of Pt electrodes was assessed *in vitro*. In order to elucidate the effects of counter-ion doping on the properties of PEDOP coatings, EDOP was polymerized in the presence of three different electrolytes, namely phosphate buffer saline (PBS), PTS and PSS. As-formed PEDOP/PBS, PEDOP/PTS and PEDOP/PSS coatings were examined in terms of their charge storage capacity, charge injection capacity, impedance, surface morphology, stability, as well as cytocompatibility with respect to a primary ventral

mesencephalic (VM) mixed cell population. Up to our knowledge, this is the first study showing the cytocompatibility evaluation of poly(3,4-ethylenedioxypyrrole) towards neural cells.

2. Experimental

2.1 Electrochemical polymerization

The process of electrochemical polymerization was performed by means of a PARSTAT 2273 potentiostat in a three-electrode set-up, comprising Pt-coated Thermanox coverslip (Electron Microscopy Sciences) as a working electrode, Ag/AgCl (3 M KCl) as a reference electrode and a glassy carbon rod as an auxiliary electrode. 10 mM 3,4-ethylenedioxypyrrole, EDOP (Sigma Aldrich, 2 % (w/v) in THF) was polymerized in a course of a cyclic voltammetry in the presence of either 1x phosphate buffer solution (PBS, 10 mM phosphate buffer, 2.7 mM potassium chloride, 137 mM sodium chloride, Sigma Aldrich) or 100 mM sodium *p*-toluenesulfonate (PTS, 95 %, Sigma Aldrich) or poly(sodium 4-styrenesulfonate) (PSS, average M_w = 70 000 g mol^{-1}, Sigma Aldrich) at the concentration of 100 mM with respect to a single structural unit acting as a doping ion. The ionic strengths of the solutions were as follows: 162.7 mM for PBS and 100 mM for both PTS and PSS (for PSS the ionic strength was calculated with respect to the structural unit). Cyclic voltammetric (CV) curves were collected at 100 mV s^{-1} for 50 CV cycles within the potential range individually chosen for each electrolyte basing on their electrochemical windows. The optimization protocol involved changing the oxidation potential of the polymerization process in order to form a polymer with superior electrochemical characteristics, in terms of high CSC and low impedance module at 1 kHz, as well as the mechanical stability high enough to withstand the sterilization procedure (Fig.S1-S3).

2.2 Chemical and morphological characterization

A Hitachi S-4700 Scanning Electron Microscope operating at 15 kV was used to collect SEM images. IR spectra were recorded using Varian 660-IR FT-IR Spectrometer in the range between 4000 and 600 cm^{-1} for 16 scans. Contact angle measurements onto PEDOP films were performed using DataPhysic OCA15 contact angle goniometer, and recorded at a room temperature (T ~ 20 °C) using deionized water. Contact angles were determined using the supplied software. Thickness and roughness (R_a) of samples were determined by means of a Dimension 3100 atomic force microscope operated by NanoScope IIIa controller (Digital Instruments), in a tapping mode with the use of a TESPA silicon probe (tip height 10–15 μm, tip radius <8 nm, cantilever force constant of 42 N m^{-1}).

2.3 Electrochemical characterization

A PARSTAT 2273 potentiostat was used for the electrochemical studies performed in a three-electrode set-up, comprising a bare Pt foil or PEDOP-coated Pt-covered Thermanox as a working electrode, Ag/AgCl (3 M KCl) as a reference electrode and glassy carbon rod as an auxiliary electrode. CV curves were collected in a physiologically relevant 1x PBS solution, within the potential range from −0.7 to 0.7 V (*vs.* Ag/AgCl) at 100 mV s^{-1} for 5 CV cycles. CV curves were used to determine charge storage capacity (CSC), calculated as the electric charge integrated under corresponding CV curve during one CV cycle [28], according to the formula:

$$CSC = \int_{t_1}^{t_2} I(t)dt \quad (1)$$

where t_1 is the time of beginning of CV cycle, t_2 is the time of end of CV cycle, and I is the current.

EIS spectra were collected in a 1x PBS solution within a frequency range from 100 mHz to 100 kHz, with AC amplitude of 40 mV (*vs.* Ag/AgCl) and DC potential equal to 0 V (*vs.* Ag/AgCl). The results were presented on Bode plots and compared to those of a bare Pt electrode. EIS Spectrum Analyzer 1.0 software and the Powell algorithm were used to fir the experimental data to an equivalent circuit model. Capacitances were calculated basing on the parameters of a constant phase element (CPE) according to the formula:

$$C = \frac{(Q_0 \cdot R)^{1/n}}{R} \quad (2)$$

where C is the capacitance (F), R is the film resistance (Ω), Q_0 and n are CPE parameters.

The charge injection capacity (CIC) was studied by the integration of chronoamperometric curves comprising a single biphasic potential pulse consisting of a 5 ms application of a reduction potential (−0.5 V *vs*. Ag/AgCl) followed by a 5 ms application of an oxidative potential (0.5 V *vs.* Ag/AgCl), simulating the parameters of neural stimulation [29–34].

2.4 Stability determination

The stability of the electrode performance was examined through performing 100 000 stimulation pulses and comparing first and last current curves. The initial and final CIC were calculated, and the percentage of CIC loss was determined according to the formula:

$$CIC_{loss} = \frac{CIC_{initial} - CIC_{final}}{CIC_{initial}} \cdot 100\% \quad (3)$$

2.5 Biological characterization

Primary cultures of a mixed neural population obtained from the mesencephalon of embryonic Sprague–Dawley rats were used to assess the cytocompatibility of PEDOP formulations as described previously [8,35]. Indirect double-immunofluorescent labelling was applied to visualize neuron and astrocyte cell populations [8,36]. Olympus Fluoview 1000 Confocal Microscope was used to collect the fluorescent images, which were further analyzed in terms of cell density and the average neurite length. Cell density was analyzed by counting the number of nuclei corresponding to neurons and astrocytes in an area of 211.97 μm × 211.97 μm in at least 20 random images taken from test and control groups [36]. The quantification of neurite length was performed through stereological methods as reported previously [37], and the average neurite length was calculated according to the formula [38]:

$$L = nT\frac{\pi}{2} \quad (4)$$

where: L is neurite length (μm), n is the number of times neurites intersect with grid lines, T is distance between grid lines (μm).

The biological experiments were conducted to include three biological replicas for both test and control groups. The results were expressed as the mean of the values ± standard error of the mean. A t-test was performed to determine the statistical significance ($p < 0.05$).

3. Results and Discussion

3.1 Electrochemical polymerization

As noted previously in numerous literature reports [39,40], the electrochemical properties of conducting polymers are strictly dependent on the conditions of synthesis, including the type of the doping ion. Therefore, the optimal polymerisation conditions were identified individually for PEDOP/PBS, PEDOP/PTS and PEDOP/PSS, in order to find the most

favourable potential range leading to the formation of the polymer with advantageous electrochemical performance, in terms of low impedance and high charge storage capacity (Fig.S1-S3), as well as mechanical stability high enough to withstand sterilization procedure. Fig.1A-C show the cyclic voltammetric (CV) curves of the process of electropolymerization of EDOP in the presence of PBS (Fig.1A), PTS (Fig.1B) and PSS (Fig.1C) as the primary electrolytes, in the optimized range of potentials. A distinctive anodic peak associated with the oxidation of the monomer was observed in all three CV curves, with the position dependent on the reaction medium. The oxidation potential of the monomer was the lowest for both PTS and PSS (0.7 V vs. Ag/AgCl), and increased for the smallest dopants, chlorides and phosphates present in PBS (0.8 V *vs.* Ag/AgCl). The fact that the electroformation of a conducting polymer proceeds more readily in the presence of PTS and PSS than in the presence of small dopants has been already observed for EDOT [41] and explained by the activation of a surface of the electrode due to the sulfonates present in PTS and PSS. During the electropolymerization process, the current peak associated with monomer oxidation was observed to decrease due to the consumption of the monomer leading to the formation of dimers, oligomers, and, finally, polymer chains. The gradual increase in current density in the regions where oxidation and reduction reactions of PEDOP occurred confirmed the formation of conductive deposits, typical for the electropolymerization process [28]. The integration of the CV curves gave the cumulative charge (Fig.S4) – the linear increase in transferred charge showed that the electrodeposition of EDOP in either PBS, PTS or PSS is a well controlled process. The thickness of as-formed films were found to be equal to 370 ± 40 nm, 602 ± 85 nm and 254 ± 23 nm for PEDOP/PBS, PEDOP/PTS and PEDOP/PSS, respectively.

Here Figure 1

3.2 Chemical and morphological analysis

The chemical structure of PEDOP was confirmed through the FTIR analysis (Fig.S5). In all three cases, a set of peak signals characteristic for PEDOP was observed, including the stretching of C-N bond (around 1240 cm^{-1}) and stretching of C-C bond (1338 cm^{-1}) [42]. SEM micrographs of PEDOP/PBS PEDOP/PTS and PEDOP/PSS, presented in Fig.2B, indicate the effect of the dopant on the surface morphology of polymer coating. As noted previously [43,44], the incorporation of PSS into the structure of the polymer resulted in a smooth topography (R_a = 16.1 nm), due to the interactions between the polymeric dopant and the growing conducting polymer chain. It can also be inferred that positively charged PEDOP oligomers are attracted by the negatively charged structural units of PSS, resulting in the stacked arrangement of pyrrole rings, as in a case of PEDOT/PSS [45,46]. Conversely, the surface of PEDOP films doped with smaller ions (chlorides/phosphates and PTS), was composed of polymer grains regularly dispersed over the Pt surface, in a similar way as observed for PEDOT [7,24]. These matrices exhibited also high values of roughness (R_a of 96.5 nm and 215 nm for PEDOP/PBS and PEDOP/PTS, respectively), which had the effect on the wettability of the surfaces. The contact angles of water on PEDOP/PBS and PEDOP/PTS (46^o and 53^o, respectively), were higher than for PEDOP/PSS (33^o), proving the hygroscopic character of the latter derived from the hydrophilic nature of PSS [47].

The consequences of the rough and nodular morphology of PEDOP/PBS and PEDOP/PTS could include the decrease in the impedance of the coated electrodes, as it was described by Xiao et al [48]. Also Yang et al [49] reported that through differing the surface morphology of conducting polymer, it is possible to improve charge capacitance and decrease impedance. The rough morphology is important also from the point of view of cell attachment, since the rough surface of conducting polymer has been found as more suitable for establishing an

intimate interface with cells than a smooth metallic surface [50], as well as enhance cell adhesion in vitro [51,52].

Here Figure 2

3.3 Charge storage capacity

Coating with a conducting polymer has been shown to increase the surface area of an electrode, leading to an increase in charge capacitance [28], associated with a double layer formation and overdoping of the polymer in a non-Nernstian redox process [53]. High capacitances are crucial for successful neural stimulation, enabling the delivery of required amounts of charge for neural depolarisation in a safe manner [54]. The maximum amount of accumulated charge can be calculated through the integration of a CV curve of the electrode collected in a physiological electrolyte within the water window of the system [28], leading to the charge storage capacity (CSC). The corresponding CV curves of PEDOP shown in Fig.3A. indicate that undesired water electrolysis does not occur with any of the experimental PEDOP formulations within a potential range of −0.7 V to 0.7 V *vs*. Ag/AgCl. Moreover, the evident evolution in the area of the CV curves indicates an increase in CSC value of PEDOP films relative to an uncoated Pt control (Fig.3B). The overall charge capacity, calculated from CV curves recorded with a scan rate of 100 mV s^{-1}, was observed to increase from 6.94 ± 0.10 mC cm^{-2} (bare Pt) to 30.99 ± 1.74 mC cm^{-2} (PEDOP/PTS) and 26.05 ± 6.77 mC cm^{-2} (PEDOP/PSS), reaching up to 50.07 ± 6.96 mC cm^{-2} (PEDOP/PBS). These values are similar to those previously reported for PEDOT coatings (CSC between 1 and 26 mC cm^{-2}) [55–59], and PEDOT/PTS coatings (a maximum CSC of 59 mC cm^{-2}) [60]. Although using the scan rate of 100 mV s^{-1} is relevant for the comparison of CV curves with other materials, since this

scan rate is commonly used for calculating CSC and can be treated as a standard in the field of neural interfaces. However, it should be kept in mind that such fast scan rates do not fully describe the capacitive behaviour of the conducting polymer matrix. Porous electrodes, and all PEDOP formulations should be treated as this kind of material, do not follow the typical for capacitors relation between current, capacitance and scan rate (I = Cv), but their current increases at a rate proportional to a power of v [61,62]. Therefore, due to the effect of the distributed resistance of the pores, the capacitance increases with decreasing v, as can be clearly seen in Fig.3C. Furthermore, by decreasing the scan rate the transition from the purely resistive toward a purely capacitive current should be observed. While the CV curves recorded at the scan rate of 100 mV s^{-1} show the mixture of a capacitive and resistive behaviour, the CV curves recorded at 10 mV s^{-1} (Fig.3D) have more rectangular shape and mirror image symmetry, what reveals the capacitive nature of PEDOP. The observed enhanced CSC performance of PEDOP/PBS relative to both PEDOP/PTS and PEDOP/PSS may be derived from the ion exchange process that occurs when the primary dopants (PTS or PSS) are exchanged with the ions present in PBS.

Here Figure 3

3.4 Charge injection capacity

Although charge storage capacity describes the maximum amount of charge that can be stored within a polymer matrix, the charge injection capacity indicates how much charge can be delivered in a single stimulation pulse [63]. To imitate physiologically relevant stimulation conditions [29–34], the chronoamperometric curves were recorded to represent the negative-first bipolar stimulation with a potentials of –0.5 V / 0.5 V (*vs.* Ag/AgCl) delivered for 5 ms

(Fig.4A). Both the coated and bare control electrodes provided stable current characteristics, with no undesirable current fluctuations. What was evidently different for these curves is the magnitude of achievable current density, which could be expressed as charge injection capacity (CIC) (Fig.4B). Although PEDOP/PBS and PEDOP/PSS were observed to possess high CSC, these coatings possessed the lowest ability to release accumulated charge, demonstrating a CIC of 70 ± 4 μC cm^{-2} and 68 ± 2 μC cm^{-2}, respectively. Conversely, PEDOP/PTS was observed to outperform both PEDOP/PBS and PEDOP/PSS as well as bare Pt control electrodes (95 ± 7 μC cm^{-2}) with a CIC of 203 ± 24 μC cm^{-2}. The superiority of PTS as a dopant has been widely described in the literature, especially for PEDOT coatings [5,7,64], which have been observed to increase the CIC of Pt electrodes by up to two orders of magnitude [64–66]. This increase is thought to be derived from the intrinsic rough morphology of PEDOT/PTS, which increases the electroactive area of the electrode yet does not hinder the charge transfer phenomena, as is the case with larger dopants, i.e. PSS [66].

Here Figure 4

3.5 Electrochemical impedance analysis

Low electrical impedance is a necessary property of neural interface in order to facilitate the stimulation of adjacent cells without a loss in performance [35]. Conducting polymer coatings are well known for their ability to lower the impedance of bare metallic electrodes, thought to be resulting from their developed morphology [51] and increased effective surface area relative to metallic substrates [67]. A lower electrochemical impedance profile when compared with a bare Pt control electrode was noted for all PEDOP formulations (Fig.5A). It was further observed that coating of the electrode with PEDOP resulted in a decrease in the

impedance below 300 Hz irrespective of the polymer dopant. This is of primary importance for neural stimulation applications, since the majority of stimulation protocols involve the use of stimulating frequencies in the range of 50 to 300 Hz [33,34]. The shape of the impedance profile for PEDOP/PTS indicated that the mechanism of charge transfer was different than for PEDOP/PBS and PEDOP/PSS coatings. This unique behavior of PEDOP/PTS was further seen from the phase angle profile (Fig.5B), in which the position of a capacitive peak was shifted to the low frequency range, indicating that the difference in the behavior of this material was caused by its high capacitance.

A detailed investigation of PEDOP formulations was possible through the use of an equivalent circuit model for the simulaton of EIS data. As the most relevant, a modified Randles circuit was employed (Fig.5A inset), comprising a parallel combination of solution resistance (R_1), charge transfer resistance (R_1), constant phase element (CPE) and Warburg diffusion element (W) [68,69]. The model resulted in a good fit (χ^2 between $0.85 \cdot 10^{-4}$ and $7.09 \cdot 10^{-4}$) between the experimental and simulated data (Tab.1). It was shown that the solution resistance was independent of the samples. The charge transfer resistance, however, was found to be lowest for PEDOP/PBS (224 ± 7 Ω) and the highest for PEDOP/PTS (2498 ± 371 Ω), as also indicated by the impedance profiles. The high capacitance of PEDOP/PTS was proven both from the double layer capacitance, evidenced in a form of a high Warburg diffusion coefficient (1503 ± 297 W / Ω $s^{-1/2}$), as well as the capacitance of the electrode itself (8.13 ± 0.30 mF cm^{-2}). The performance of PEDOP was found to outperform its structural analogues, namely PPy (R = 6.6 ± 0.1 kΩ, C = 6.6 ± 0.2 μF cm^{-2}) [70] and PEDOT (R = 4.2 ± 0.3 kΩ, C = 13.8 ± 0.1 μF cm^{-2}) [70]. When the thickness of PEDOP films was taken into account, the volumetric capacitance of PEDOP/PTS reached a value of 135 F cm^{-3}, which is still much higher than for both PEDOP/PBS (2.7 F cm^{-3}) and PEDOP/PTS (3.1 F cm^{-3}), greatly exceeding the volumetric capacitance determined for PEDOT/PSS (39 F cm^{-3}) [71].

Here Figure 5 and Table 1

3.6 Stability determination

To evaluate the stability of all experimental polymer coatings, PEDOP/PBS, PEDOP/PTS and PEDOP/PSS, as well as bare Pt electrodes, were subjected to 100 000 stimulation pulses (Fig.S6). The maximum current densities of the positive pulse (Fig.6A) were constant over the duration of the experiment. To provide qualitative data, CIC values were calculated for the first and last stimulation pulses, and the loss in CIC was determined (Fig.6B). The highest loss in CIC (9.4 ± 0.9 %) was noted for the bare Pt electrodes, indicating that even unmodified noble metal electrodes are prone to a loss in electroactivity, as observed previously [7]. Coating with a conducting polymer layer greatly increased the stability of the electrode, with maximum stability observed for PEDOP/PTS coatings (CIC loss of only 0.49 ± 0.06 %). The superior stability of conducting polymers doped with PTS has been already reported for PEDOT/PTS materials [5,64]. Furthermore, PEDOT/PTS coatings have been noted previously for possessing a high adherence to Pt substrates [72], a high stability when exposed to various solvents [73] and when subjected to the electrochemical doping and de-doping processes [74], occurring during neural stimulation. PEDOT/PTS was also found to withstand accelerated material aging as well as steam sterilization [75]. This stability of PEDOT/PTS has been found to be significantly greater than that of PEDOT/PSS, which has been extensively explored in the field of neural engineering [64]. Our results indicate that the choice of the dopant has a significant effect also for PEDOP coatings, here demonstrating that PEDOP/PTS formulations outperformed both PEDOP/PBS and PEDOP/PSS in terms of stability, a primary concern for the design of neural interface with chronic applications.

Here Figure 6

3.7 Cytocompatibility

To assess the suitability of PEDOP coatings as a neural interface material, a primary ventral mesencephalic (VM) mixed cell population was cultured on PEDOP-coated electrodes for 3, 7 and 14 days. At each time-point, the cells were fixed and immunostained with DAPI for cell nuclei, anti-β III tubulin for neurons and anti-GFAP for astrocytes (Fig.7A). The fluorescent images were then quantified to estimate the neuron-to-astrocyte ratio (Fig.7B) and the average neurite length (Fig.7C). The neural-to-astrocyte ratio, which is used to assess the cytocompatibility of a material *in vitro* to neural systems [36], showed the prevalence of neurons after 3 days in culture for all PEDOP formulations when compared to Pt control substrates. This indicated that the polymer surface promoted neuronal adhesion and viability, as described in previous studies for other types of electrode modifications [76,77]. After 7 days, the ratio of astrocytes to neurons was normalized with no significant differences between all experimental groups. Following 14 days of culture, the percentage of neurons was lower for PEDOP/PSS when compared with PEDOP/PBS and PEDOP/PTS, which may indicate that this surface has lower cytocompatibility. This observation was supported by an analysis of the average neurite length, which was lower for PEDOP/PSS (842 ± 8 μm) when compared with other polymer coatings, but still greater when compared with bare Pt (370 ± 4 μm). The most extensive neuron outgrowth was noted with both PEDOP/PBS and PEDOP/PTS coatings, for which the average neurite length after 14 days in culture was 1095 ± 40 μm and 1116 ± 20 μm, respectively. The results clearly indicate the ability of all PEDOP formulations to enhance the process of neuron growth, with the most advantageous effect provided by PEDOP/PTS. The major restraint limiting the use of PEDOP in biomedical

applications has been overcome by showing that not only it does not have the adverse effects on neural cells, but also promotes the outgrowth of neurons and favours the "healthy" ratio between neurons and astrocytes. Confirmed cytocompatibility of PEDOP towards neural cells opens the way of the application of this material in a new, biomedical context. Therefore, PEDOP can now be considered as a promising alternative to PPy and PEDOT in the field of neural science.

Here Figure 7

4. Conclusions

In this study, the applicability of a poly(3,4-ethylenedioxypyrrole) (PEDOP) as a neural interface biomaterial was assessed *in vitro*. The electrochemical and biological performance of PEDOP was found out to be dependent on the electrolyte solution, showing the superiority of *p*-toluenesulfonate (PTS) as a dopant. Due to the strong interactions between PTS and the growing polymer chain, it was possible to form a good quality PEDOP coating at low oxidation potentials (0.7 V *vs.* Ag/AgCl). PEDOP/PTS was found to exhibit promising surface morphology influencing the capacitance of the coating as well as cell adhesion. Even though possessing a medium CSC (30.99 ± 1.74 mC cm^{-2}), PEDOP/PTS was able to release substantial amounts of charge under stimulating conditions (CIC of 203 ± 24 μC cm^{-2}) with only a slight decrease in performance (CIC loss of 0.49 ± 0.06 % after 100 000 stimulation pulses). Moreover, the coating of Pt electrodes with PEDOP resulted in a significant decrease in the impedance profile at physiologically relevant frequencies (< 300 Hz). After confirming the beneficial electrochemical properties of PEDOP films, these materials were assessed in terms of their cytocompatiblity and were shown to enhance neurite extension in mixed neuron

populations after 14 days in culture. Neurite length was observed to increase from 370 ± 4 μm to 1116 ± 20 μm and in cells cultured on bare Pt control and PEDOP/PTS coated Pt substrates respectively. Unprecedented in the literature, our results proved that PEDOP not only does not have the adverse effects on neural cells, but also promotes the outgrowth of neurons and favours the "healthy" ratio between neurons and astrocytes. Consequently, PEDOP, and in particular PEDOP/PTS, was shown to serve as a robust neural interface material, possessing favourable electrochemical characteristics together with high neural cytocompatibility. Therefore, we believe that our studies have led to the expansion of the current library of conducting polymers exhibiting cytocompatibility by a new member.

Acknowledgements

This publication has emanated from research conducted with the financial support of Science Foundation Ireland (SFI) and is co-funded under the European Regional Development Fund under Grant Number 13/RC/2073. This project has received funding from the European Union's Horizon 2020 research and innovation programme under the Marie Skłodowska-Curie grant agreement No 713690 and SFI Technology Innovation Development Programme, grant no. 15/TIDA/2992. This work has been supported by the Polish National Science Centre in the framework of Sonata 2016/23/D/ST5/01306. The authors acknowledge the facilities and scientific and technical assistance of the Centre for Microscopy & Imaging at the National University of Ireland Galway, a facility that is funded by NUIG and the Irish Government's Programme for Research in Third Level Institutions, Cycles 4 and 5, National Development Plan 2007-2013.

References

[1] N.K. Guimard, N. Gomez, C.E. Schmidt, Conducting polymers in biomedical engineering, Prog. Polym. Sci. 32 (2007) 876–921. doi:10.1016/j.progpolymsci.2007.05.012.

[2] R. Langer, Biomaterials and biomedical engineering, Chem. Eng. Sci. 50 (1995) 4109–4121. doi:10.1016/0009-2509(95)00226-X.

[3] A.G. MacDiarmid, "Synthetic metals": A novel role for organic polymers (Nobel lecture), Angew. Chemie - Int. Ed. 40 (2001) 2581–2590. doi:10.1002/1521-3773(20010716)40:14<2581::AID-ANIE2581>3.0.CO;2-2.

[4] T.F. Otero, J.M. Sansiñena, Soft and wet conducting polymers for artificial muscles, Adv. Mater. 10 (1998) 491–494. doi:10.1002/(SICI)1521-4095(199804)10:6<491::AID-ADMA491>3.0.CO;2-Q.

[5] R.A. Green, N.H. Lovell, G.G. Wallace, L.A. Poole-Warren, Conducting polymers for neural interfaces: Challenges in developing an effective long-term implant, Biomaterials. 29 (2008) 3393–3399. doi:10.1016/j.biomaterials.2008.04.047.

[6] C. Vallejo-Giraldo, A. Kelly, M.J.P. Biggs, Biofunctionalisation of electrically conducting polymers, Drug Discov. Today. 19 (2014) 88–94. doi:10.1016/j.drudis.2013.07.022.

[7] C. Vallejo-Giraldo, K. Krukiewicz, I. Calaresu, J. Zhu, M. Palma, M. Fernandez-Yague, B.W. McDowell, N. Peixoto, N. Farid, G. O'Connor, L. Ballerini, A. Pandit, M.J.P. Biggs, Attenuated Glial Reactivity on Topographically Functionalized Poly(3,4-Ethylenedioxythiophene):P-Toluene Sulfonate (PEDOT:PTS) Neuroelectrodes Fabricated by Microimprint Lithography, Small. 14 (2018) 1800863. doi:10.1002/smll.201800863.

[8] K. Krukiewicz, M. Chudy, C. Vallejo-Giraldo, M. Skorupa, D. Więcławska, R. Turczyn, M. Biggs, Fractal form PEDOT/Au assemblies as thin-film neural interface materials, Biomed. Mater. 13 (2018) 54102. http://stacks.iop.org/1748-605X/13/i=5/a=054102.

[9] A. Kassim, Z.B. Basar, H.N.M.E. Mahmud, Effects of preparation temperature on the conductivity of polypyrrole conducting polymer, Proc. Indian Acad. Sci. Chem. Sci. 114 (2002) 155–162. doi:10.1007/BF02704308.

[10] Z.B. Huang, G.F. Yin, X.M. Liao, J.W. Gu, Conducting polypyrrole in tissue engineering applications, Front. Mater. Sci. 8 (2014) 39–45. doi:10.1007/s11706-014-0238-8.

[11] L. Valero, J. Arias-Pardilla, J. Cauich-Rodríguez, M.A. Smit, T.F. Otero, Characterization of the movement of polypyrrole-dodecylbenzenesulfonate-perchlorate/tape artificial muscles. Faradaic control of reactive artificial molecular motors and muscles, Electrochim. Acta. 56 (2011) 3721–3726. doi:10.1016/j.electacta.2010.11.058.

[12] K. Krukiewicz, A. Stokfisz, J.K. Zak, Two approaches to the model drug immobilization into conjugated polymer matrix., Mater. Sci. Eng. C. Mater. Biol. Appl. 54 (2015) 176–181. doi:10.1016/j.msec.2015.05.017.

[13] P.M. George, A.W. Lyckman, D.A. Lavan, A. Hegde, Y. Leung, R. Avasare, C. Testa, P.M. Alexander, R. Langer, M. Sur, Fabrication and biocompatibility of polypyrrole implants suitable for neural prosthetics, Biomaterials. 26 (2005) 3511–3519.

doi:10.1016/j.biomaterials.2004.09.037.

[14] R. Ravichandran, S. Sundarrajan, J.R. Venugopal, S. Mukherjee, S. Ramakrishna, Applications of conducting polymers and their issues in biomedical engineering, J. R. Soc. Interface. 7 (2010) 559–579. doi:10.1098/rsif.2010.0120.focus.

[15] T. Boretius, M. Schuettler, T. Stieglitz, On the Stability of Poly-Ethylenedioxythiopene as Coating Material for Active Neural Implants, Artif. Organs. 35 (2011) 245–248. doi:10.1111/j.1525-1594.2011.01210.x.

[16] P. Schottland, K. Zong, C.L. Gaupp, B.C. Thompson, C.A. Thomas, I. Giurgiu, R. Hickman, K.A. Abboud, J.R. Reynolds, Poly(3,4-alkylenedioxypyrrole)s: Highly stable electronically conducting and electrochromic polymers, Macromolecules. 33 (2000) 7051–7061. doi:10.1021/ma000490f.

[17] K. Krukiewicz, T. Jarosz, A.P. Herman, R. Turczyn, S. Boncel, J.K. Zak, The effect of solvent on the synthesis and physicochemical properties of poly(3,4-ethylenedioxypyrrole), Synth. Met. 217 (2016) 231–236. doi:10.1016/j.synthmet.2016.04.005.

[18] S.K. Kim, Y.N. Jeong, M.S. Ahmed, J.M. You, H.C. Choi, S. Jeon, Electrocatalytic determination of hydrazine by a glassy carbon electrode modified with PEDOP/MWCNTs-Pd nanoparticles, Sensors Actuators, B Chem. 153 (2011) 246–251. doi:10.1016/j.snb.2010.10.039.

[19] Ö. Türkarslan, A.E. Böyükbayram, L. Toppare, Amperometric alcohol biosensors based on conducting polymers: Polypyrrole, poly(3,4-ethylenedioxythiophene) and poly(3,4-ethylenedioxypyrrole), Synth. Met. 160 (2010) 808–813. doi:10.1016/j.synthmet.2010.01.027.

[20] K. Krukiewicz, P. Zawisza, A.P. Herman, R. Turczyn, S. Boncel, J.K. Zak, An electrically controlled drug delivery system based on conducting poly(3,4-ethylenedioxypyrrole) matrix, Bioelectrochemistry. 108 (2016) 13–20. doi:10.1016/j.bioelechem.2015.11.002.

[21] R.M. Walczak, J.R. Reynolds, Poly(3,4-alkylenedioxypyrroles): The PXDOPs as versatile yet underutilized electroactive and conducting polymers, Adv. Mater. 18 (2006) 1121–1131. doi:10.1002/adma.200502312.

[22] S. Sinha, S. Bhadra, D. Khastgir, Effect of dopant type on the properties of polyaniline, J. Appl. Polym. Sci. 112 (2009) 3135–3140. doi:10.1002/app.29708.

[23] G. Sabouraud, S. Sadki, N. Brodie, The mechanisms of pyrrole electropolymerization, Chem. Soc. Rev. 29 (2000) 283–293. doi:10.1039/a807124a.

[24] K. Krukiewicz, A. Kruk, R. Turczyn, Evaluation of drug loading capacity and release characteristics of PEDOT/naproxen system: Effect of doping ions, Electrochim. Actarochimica Acta. 289 (2018) 218–227.

[25] L.F. Warren, J.A. Walker, D.P. Anderson, C.G. Rhodes, L.J. Buckley, A study of conducting polymer morphology - The effect of dopant anions upon order, J. Electrochem. Soc. 136 (1989) 2286–2295. doi:10.1149/1.2097303.

[26] S. Baek, R.A. Green, L.A. Poole-Warren, Effects of dopants on the biomechanical properties of conducting polymer films on platinum electrodes, J. Biomed. Mater. Res. - Part A. 102 (2014) 2743–2754. doi:10.1002/jbm.a.34945.

[27] F. Pires, Q. Ferreira, C.A.V. Rodrigues, J. Morgado, F.C. Ferreira, Neural stem cell

differentiation by electrical stimulation using a cross-linked PEDOT substrate: Expanding the use of biocompatible conjugated conductive polymers for neural tissue engineering, Biochim. Biophys. Acta. 1850 (2015) 1158–1168. doi:10.1016/j.bbagen.2015.01.020.

[28] K. Krukiewicz, J.K. Zak, Conjugated polymers as robust carriers for controlled delivery of anti-inflammatory drugs, J. Mater. Sci. 49 (2014) 5738–5745. doi:10.1007/s10853-014-8292-2.

[29] D.R. Merrill, M. Bikson, J.G.R. Jefferys, Electrical stimulation of excitable tissue: Design of efficacious and safe protocols, J. Neurosci. Methods. (2005) 171–198. doi:10.1016/j.jneumeth.2004.10.020.

[30] U. Akbar, R.S. Raike, N. Hack, C.W. Hess, J. Skinner, D. Martinez-Ramirez, S. DeJesus, M.S. Okun, Randomized, Blinded Pilot Testing of Nonconventional Stimulation Patterns and Shapes in Parkinson's Disease and Essential Tremor: Evidence for Further Evaluating Narrow and Biphasic Pulses, Neuromodulation. 19 (2016) 343–356. doi:10.1111/ner.12397.

[31] A. Eusebio, W. Thevathasan, L. Doyle Gaynor, A. Pogosyan, E. Bye, T. Foltynie, L. Zrinzo, K. Ashkan, T. Aziz, P. Brown, Deep brain stimulation can suppress pathological synchronisation in parkinsonian patients, J. Neurol. Neurosurg. Psychiatry. 82 (2011) 569–573. doi:10.1136/jnnp.2010.217489.

[32] C.R. Butson, C.C. McIntyre, Tissue and electrode capacitance reduce neural activation volumes during deep brain stimulation, Clin. Neurophysiol. 116 (2005) 16125463. doi:10.1016/j.clinph.2005.06.023.

[33] A.L. Benabid, P. Pollak, D. Gao, D. Hoffmann, P. Limousin, E. Gay, I. Payen, A. Benazzouz, Chronic electrical stimulation of the ventralis intermedius nucleus of the thalamus as a treatment of movement disorders, J. Neurosurg. 84 (1996) 203–214. doi:10.3171/jns.1996.84.2.0203.

[34] C.C. McIntyre, W.M. Grill, Extracellular stimulation of central neurons: influence of stimulus waveform and frequency on neuronal output., J. Neurophysiol. 88 (2002) 1592–1604. doi:DOI 10.1152/jn.00147.2002.

[35] C. Vallejo-Giraldo, N.P. Pampaloni, A.R. Pallipurath, P. Mokarian-Tabari, J. O'Connell, J.D. Holmes, A. Trotier, K. Krukiewicz, G. Orpella-Aceret, E. Pugliese, L. Ballerini, M. Kilcoyne, E. Dowd, L.R. Quinlan, A. Pandit, P. Kavanagh, M.J.P. Biggs, Preparation of Cytocompatible ITO Neuroelectrodes with Enhanced Electrochemical Characteristics Using a Facile Anodic Oxidation Process, Adv. Funct. Mater. 28 (2017) 1605035. doi:10.1002/adfm.201605035.

[36] C. Vallejo-Giraldo, E. Pugliese, A. Larrañaga, M.A. Fernandez-Yague, J.J. Britton, A. Trotier, G. Tadayyon, A. Kelly, I. Rago, J.R. Sarasua, E. Dowd, L.R. Quinlan, A. Pandit, M.J.P. Biggs, Polyhydroxyalkanoate/carbon nanotube nanocomposites: Flexible electrically conducting elastomers for neural applications, Nanomedicine. 11 (2016) 2547–2563. doi:10.2217/nnm-2016-0075.

[37] G.W. O'Keeffe, P. Dockery, A.M. Sullivan, Effects of growth/differentiation factor 5 on the survival and morphology of embryonic rat midbrain dopaminergic neurones in vitro, J. Neurocytol. 33 (2004) 479–488. doi:10.1007/s11068-004-0511-y.

[38] E.T. Kavanagh, J.P. Loughlin, K.R. Herbert, P. Dockery, A. Samali, K.M. Doyle, A.M. Gorman, Functionality of NGF-protected PC12 cells following exposure to 6-

hydroxydopamine, Biochem. Biophys. Res. Commun. 351 (2006) 890–895. doi:10.1016/j.bbrc.2006.10.104.

[39] B. Krische, M. Zagorska, Overoxidation in conducting polymers, Synth. Met. 28 (1989) 257–262. doi:10.1016/0379-6779(89)90530-4.

[40] G.G. Wallace, M. Smyth, H. Zhao, Conducting electroactive polymer-based biosensors, TrAC - Trends Anal. Chem. 18 (1999) 245–251. doi:10.1016/S0165-9936(98)00113-7.

[41] J. Xia, N. Masaki, K. Jiang, S. Yanagida, The influence of doping ions on poly(3,4-ethylenedioxythiophene) as a counter electrode of a dye-sensitized solar cell, J. Mater. Chem. 17 (2007) 2845–2850. doi:10.1039/b703062b.

[42] B.N. Reddy, M. Deepa, Electrochromic switching and nanoscale electrical properties of a poly(5-cyano indole)-poly(3,4-ethylenedioxypyrrole) device with a free standing ionic liquid electrolyte, Polym. (United Kingdom). 54 (2013) 5801–5811. doi:10.1016/j.polymer.2013.08.016.

[43] M. Sain, S. Ummartyotin, J. Juntaro, C. Wu, H. Manuspiya, Deposition of PEDOT: PSS nanoparticles as a conductive microlayer anode in OLEDs device by desktop inkjet printer, J. Nanomater. (2011) 606714. doi:10.1155/2011/606714.

[44] C. Pirvu, C.C. Manole, Electrochemical surface plasmon resonance for in situ investigation of antifouling effect of ultra thin hybrid polypyrrole/PSS films, Electrochim. Acta. 89 (2013) 63–71. doi:10.1016/j.electacta.2012.11.045.

[45] A.W.M. Diah, J.P. Quirino, W. Belcher, C.I. Holdsworth, Investigation of the doping efficiency of poly(styrene sulfonic acid) in poly(3,4-ethylenedioxythiophene)/poly(styrene sulfonic acid) dispersions by capillary electrophoresis, Electrophoresis. 35 (2014) 1976–1983. doi:10.1002/elps.201400056.

[46] S. Kirchmeyer, K. Reuter, Scientific importance, properties and growing applications of poly(3,4-ethylenedioxythiophene), J. Mater. Chem. 15 (2005) 2077–2088. doi:10.1039/b417803n.

[47] M. Döbbelin, R. Marcilla, M. Salsamendi, C. Pozo-Gonzalo, P.M. Carrasco, J.A. Pomposo, D. Mecerreyes, Influence of ionic liquids on the electrical conductivity and morphology of PEDOT:PSS films, Chem. Mater. 20 (2007) 7613–7622. doi:10.1021/cm070398z.

[48] Y. Xiao, X. Cui, J.M. Hancock, M. Bouguettaya, J.R. Reynolds, D.C. Martin, Electrochemical polymerization of poly(hydroxymethylated-3,4-ethylenedioxythiophene) (PEDOT-MeOH) on multichannel neural probes, Sensors Actuators, B Chem. 99 (2004) 437–443. doi:10.1016/j.snb.2003.12.067.

[49] J. Yang, D.H. Kim, J.L. Hendricks, M. Leach, R. Northey, D.C. Martin, Ordered surfactant-templated poly(3,4-ethylenedioxythiophene) (PEDOT) conducting polymer on microfabricated neural probes, Acta Biomater. 1 (2005) 125–136. doi:10.1016/j.actbio.2004.09.006.

[50] L.J. del Valle, D. Aradilla, R. Oliver, F. Sepulcre, A. Gamez, E. Armelin, C. Alemán, F. Estrany, Cellular adhesion and proliferation on poly(3,4-ethylenedioxythiophene): Benefits in the electroactivity of the conducting polymer, Eur. Polym. J. 43 (2007) 2342–2349. doi:10.1016/j.eurpolymj.2007.03.050.

[51] X. Cui, D.C. Martin, Fuzzy gold electrodes for lowering impedance and improving adhesion with electrodeposited conducting polymer films, Sensors Actuators, A Phys.

103 (2003) 384–394. doi:10.1016/S0924-4247(02)00427-2.

[52] M. Bongo, O. Winther-Jensen, S. Himmelberger, X. Strakosas, M. Ramuz, A. Hama, E. Stavrinidou, G.G. Malliaras, A. Salleo, B. Winther-Jensen, R.M. Owens, PEDOT:gelatin composites mediate brain endothelial cell adhesion, J. Mater. Chem. B. 1 (2013) 3860–3867. doi:10.1039/c3tb20374c.

[53] J. Tanguy, N. Mermilliod, M. Hoclet, Capacitive Charge and Noncapacitive Charge in Conducting Polymer Electrodes, J. Electrochem. Soc. 134 (1987) 795–802. doi:10.1149/1.2100575.

[54] C.S. Alex Gong, W.J. Syu, K.F. Lei, Y.S. Hwang, Development of a flexible non-metal electrode for cell stimulation and recording, Sensors (Switzerland). 16 (2016) 1613. doi:10.3390/s16101613.

[55] Z.A. King, C.M. Shaw, S.A. Spanninga, D.C. Martin, Structural, chemical and electrochemical characterization of poly(3,4-Ethylenedioxythiophene) (PEDOT) prepared with various counter-ions and heat treatments, Polymer (Guildf). 52 (2011) 1302–1308. doi:10.1016/j.polymer.2011.01.042.

[56] M. Ganji, A. Tanaka, V. Gilja, E. Halgren, S.A. Dayeh, Scaling Effects on the Electrochemical Stimulation Performance of Au, Pt, and PEDOT:PSS Electrocorticography Arrays, Adv. Funct. Mater. 27 (2017) 1703019. doi:10.1002/adfm.201703019.

[57] Z.J. Du, X. Luo, C.L. Weaver, X.T. Cui, Poly(3,4-ethylenedioxythiophene)-ionic liquid coating improves neural recording and stimulation functionality of MEAs, J. Mater. Chem. C. 3 (2015) 6515–6524. doi:10.1039/c5tc00145e.

[58] K. Wang, R.Y. Tang, X.B. Zhao, J.J. Li, Y.R. Lang, X.X. Jiang, H.J. Sun, Q.X. Lin, C.Y. Wang, Covalent bonding of YIGSR and RGD to PEDOT/PSS/MWCNT-COOH composite material to improve the neural interface, Nanoscale. 7 (2015) 18677–18685. doi:10.1039/c5nr05784a.

[59] C. Kleber, M. Bruns, K. Lienkamp, J. Rühe, M. Asplund, An interpenetrating, microstructurable and covalently attached conducting polymer hydrogel for neural interfaces, Acta Biomater. 58 (2017) 365–375. doi:10.1016/j.actbio.2017.05.056.

[60] H.C. Tian, J.Q. Liu, X.Y. Kang, Q. He, B. Yang, X. Chen, C.S. Yang, Flexible multi-channel microelectrode with fluidic paths for intramuscular stimulation and recording, Sensors Actuators, A Phys. 228 (2015) 28–39. doi:10.1016/j.sna.2015.02.035.

[61] W.G. Pell, B.E. Conway, Voltammetry at a de Levie brush electrode as a model for electrochemical supercapacitor behaviour, J. Electroanal. Chem. 500 (2001) 121–133. doi:10.1016/S0022-0728(00)00423-X.

[62] W.G. Pell, B.E. Conway, N. Marincic, Analysis of non-uniform charge/discharge and rate effects in porous carbon capacitors containing sub-optimal electrolyte concentrations, J. Electroanal. Chem. 491 (2000) 9–21. doi:10.1016/S0022-0728(00)00207-2.

[63] E.M. Hudak, D.W. Kumsa, H.B. Martin, J.T. Mortimer, Electron transfer processes occurring on platinum neural stimulating electrodes: Calculated charge-storage capacities are inaccessible during applied stimulation, J. Neural Eng. 14 (2017) 046012. doi:10.1088/1741-2552/aa6945.

[64] R.A. Green, P.B. Matteucci, R.T. Hassarati, B. Giraud, C.W.D. Dodds, S. Chen, P.J. Byrnes-Preston, G.J. Suaning, L.A. Poole-Warren, N.H. Lovell, Performance of

conducting polymer electrodes for stimulating neuroprosthetics, J. Neural Eng. 10 (2013) 016009. doi:10.1088/1741-2560/10/1/016009.

[65] S.F. Cogan, Neural Stimulation and Recording Electrodes, Annu. Rev. Biomed. Eng. 10 (2008) 275–309. doi:10.1146/annurev.bioeng.10.061807.160518.

[66] U.A. Aregueta-Robles, A.J. Woolley, L.A. Poole-Warren, N.H. Lovell, R.A. Green, Organic electrode coatings for next-generation neural interfaces, Front. Neuroeng. 7 (2014) 15. doi:10.3389/fneng.2014.00015.

[67] M.R. Abidian, J.M. Corey, D.R. Kipke, D.C. Martin, Conducting-polymer nanotubes improve electrical properties, mechanical adhesion, neural attachment and neurite outgrowth of neural electrodes, Small. 6 (2010) 421–429. doi:10.1002/smll.200901868.

[68] P. A. Basnayaka, M. K. Ram, L. Stefanakos, A. Kumar, Graphene/Polypyrrole Nanocomposite as Electrochemical Supercapacitor Electrode: Electrochemical Impedance Studies, Graphene. 2 (2013) 81–87. doi:10.4236/graphene.2013.22012.

[69] Y. Braham, H. Barhoumi, A. Maaref, A. Bakhrouf, C.G. Heywang, T.C. Bouhacina, N. Jaffrezic-Renault, Characterization of Urea Biosensor Based on the Immobilization of Bacteria Proteus Mirabilis in Interaction with Iron Oxide Nanoparticles on Gold Electrode, J. Biosens. Bioelectron. 6 (2015) 100016. doi: 10.4172/2155-6210.1000160.

[70] M.R. Abidian, D.C. Martin, Experimental and theoretical characterization of implantable neural microelectrodes modified with conducting polymer nanotubes, Biomaterials. 29 (2008) 1273–1283. doi:10.1016/j.biomaterials.2007.11.022.

[71] C.M. Proctor, J. Rivnay, G.G. Malliaras, Understanding volumetric capacitance in conducting polymers, J. Polym. Sci. Part B Polym. Phys. 54 (2016) 1433–1436. doi:10.1002/polb.24038.

[72] R.A. Green, R.T. Hassarati, J.A. Goding, S. Baek, N.H. Lovell, P.J. Martens, L.A. Poole-Warren, Conductive Hydrogels: Mechanically Robust Hybrids for Use as Biomaterials, Macromol. Biosci. 12 (2012) 494–501. doi:10.1002/mabi.201100490.

[73] V. Armel, J. Rivnay, G. Malliaras, B. Winther-Jensen, Unexpected interaction between PEDOT and phosphonium ionic liquids, J. Am. Chem. Soc. 135 (2013) 11309–11313. doi:10.1021/ja405032c.

[74] K.E. Aasmundtveit, E.J. Samuelsen, O. Inganäs, L.A.A. Pettersson, T. Johansson, S. Ferrer, Structural aspects of electrochemical doping and dedoping of poly(3,4-ethylenedioxythiophene), Synth. Met. 113 (2000) 93. doi:10.1016/S0379-6779(00)00181-8.

[75] R.A. Green, R.T. Hassarati, L. Bouchinet, C.S. Lee, G.L.M. Cheong, J.F. Yu, C.W. Dodds, G.J. Suaning, L.A. Poole-Warren, N.H. Lovell, Substrate dependent stability of conducting polymer coatings on medical electrodes, Biomaterials. 33 (2012) 5875–5886. doi:10.1016/j.biomaterials.2012.05.017.

[76] T. Gabay, E. Jakobs, E. Ben-Jacob, Y. Hanein, Engineered self-organization of neural networks using carbon nanotube clusters, Phys. A Stat. Mech. Its Appl. 350 (2005) 611–621. doi:10.1016/j.physa.2004.11.007.

[77] P. Roach, T. Parker, N. Gadegaard, M.R. Alexander, Surface strategies for control of neuronal cell adhesion: A review, Surf. Sci. Rep. 65 (2010) 145–173. doi:10.1016/j.surfrep.2010.07.001.

Figures and captions

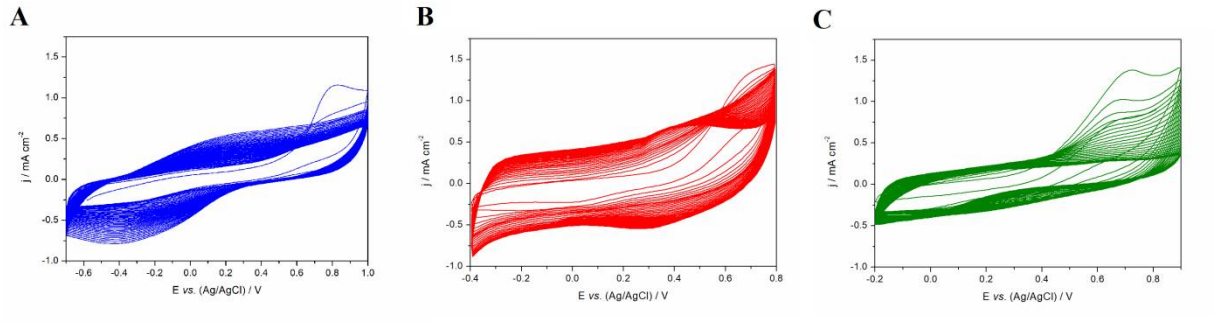

Fig.1. CV curves recorded during the electrochemical polymerisation of 10 mM EDOP in the presence of 1x PBS (A), 0.1 M PTS (B) and 0.1 M PSS (C); scan rate 100 mV s^{-1}, 50 CV cycles.

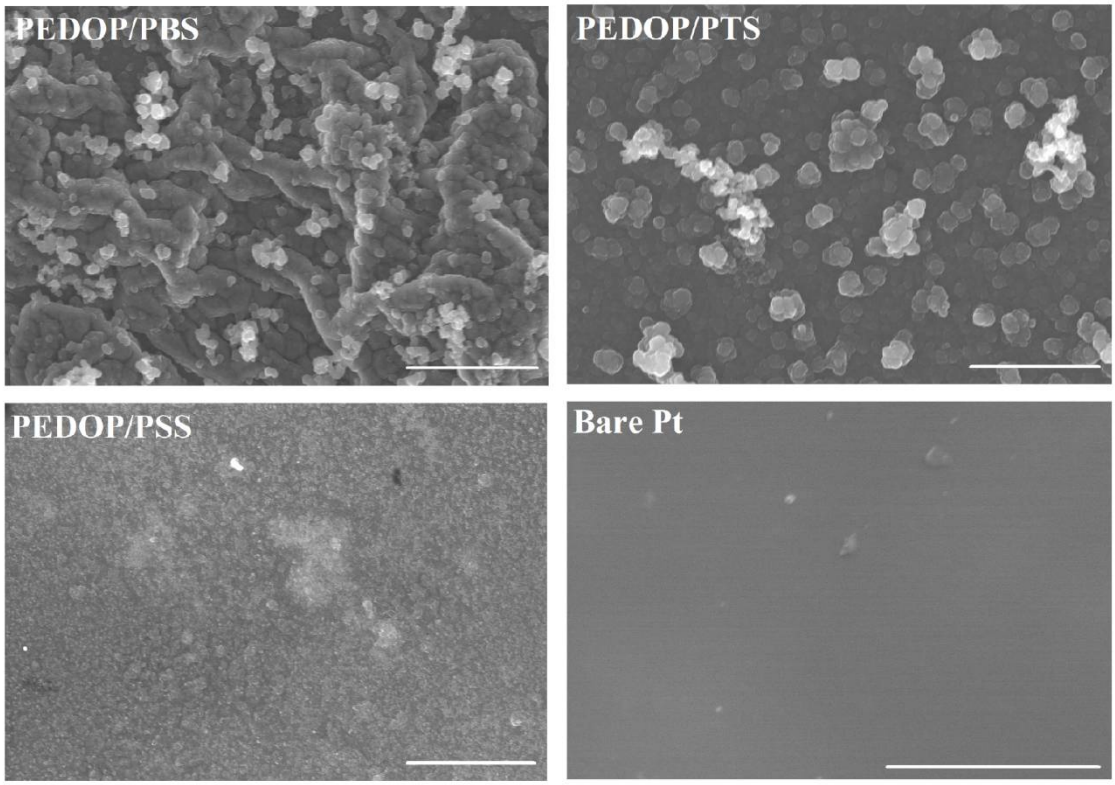

Fig.2. SEM micrographs of PEDOP/PBS, PEDOP/PTS and PEDOP/PSS matrices electrodeposited onto Pt macroelectrodes, as well as bare Pt; scale bar represents 10 μm.

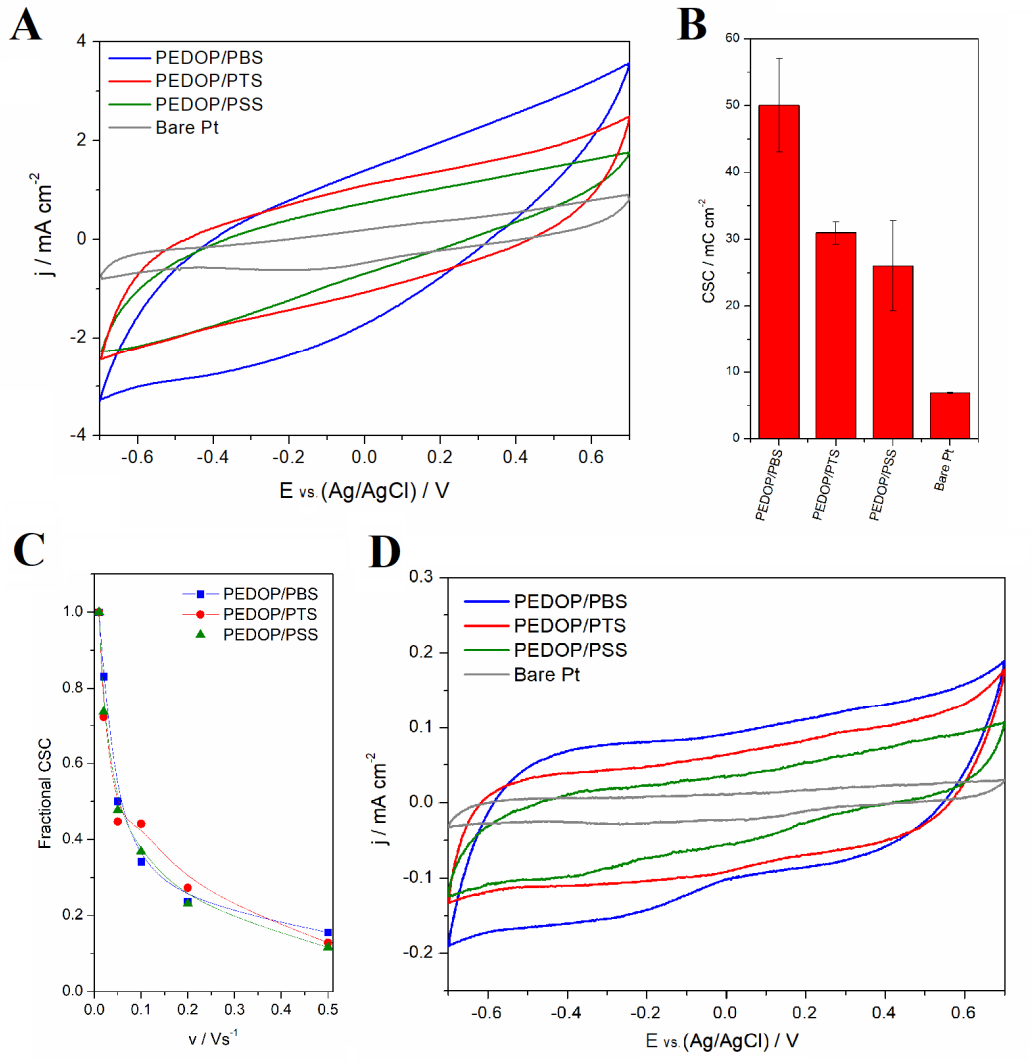

Fig.3. Cyclic voltammetric curves recorded at 100 mV s^{-1} (A), charge storage capacity (CSC) values calculated for the scan rate of 100 mV s^{-1} (B), fractional CSC relative to that for v = 10 mV s^{-1} (C) and cyclic voltammetric curves recorded at 10 mV s^{-1} (D) of Pt electrodes coated with PEDOP/PBS, PEDOP/PTS and PEDOP/PSS as well as a bare Pt electrode; $N = 3$.

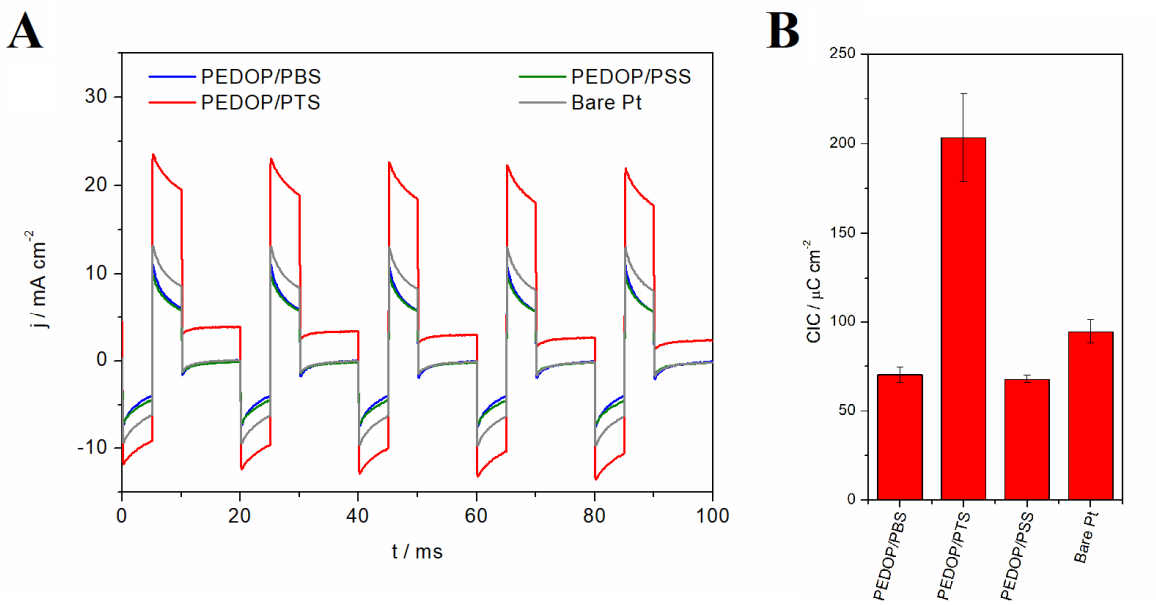

Fig.4. Chronoamperometric curves (A) and charge injection capacity (CIC) values (B) of Pt electrodes coated with PEDOP/PBS, PEDOP/PTS and PEDOP/PSS as well as bare Pt control electrodes; $N = 3$.

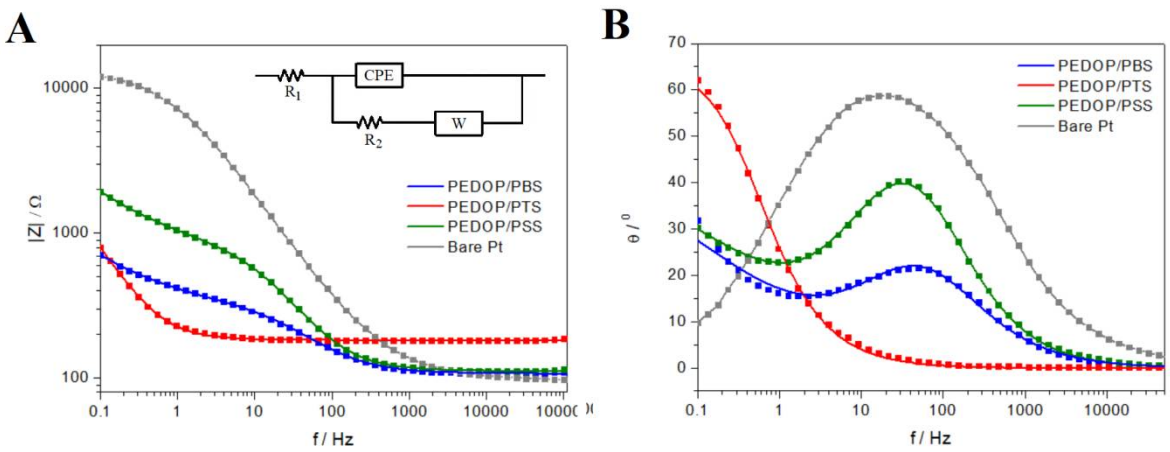

Fig.5. Electrochemical impedance spectroscopy data in the form of Bode plots showing the frequency-dependent behaviour of the impedance modulus (A) and phase angle (B) of Pt electrodes coated with PEDOP/PBS, PEDOP/PTS and PEDOP/PSS as well as bare Pt electrodes; equivalent circuit are presented as an inset; dots represent experimental data, while lines represent simulated results.

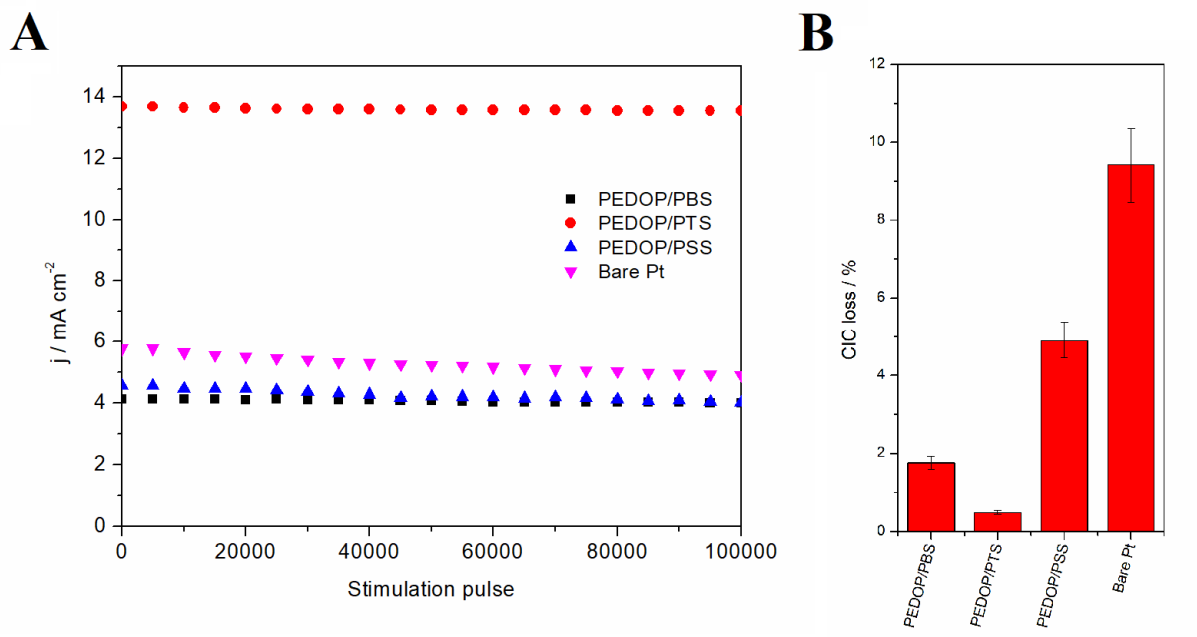

Fig.6. The maximum current densities recorded following the subjection of PEDOP-coated, and bare Pt control electrodes, to 100 000 stimulation pulses (A), the percentage loss in CIC during stability evaluation (B); $N = 3$.

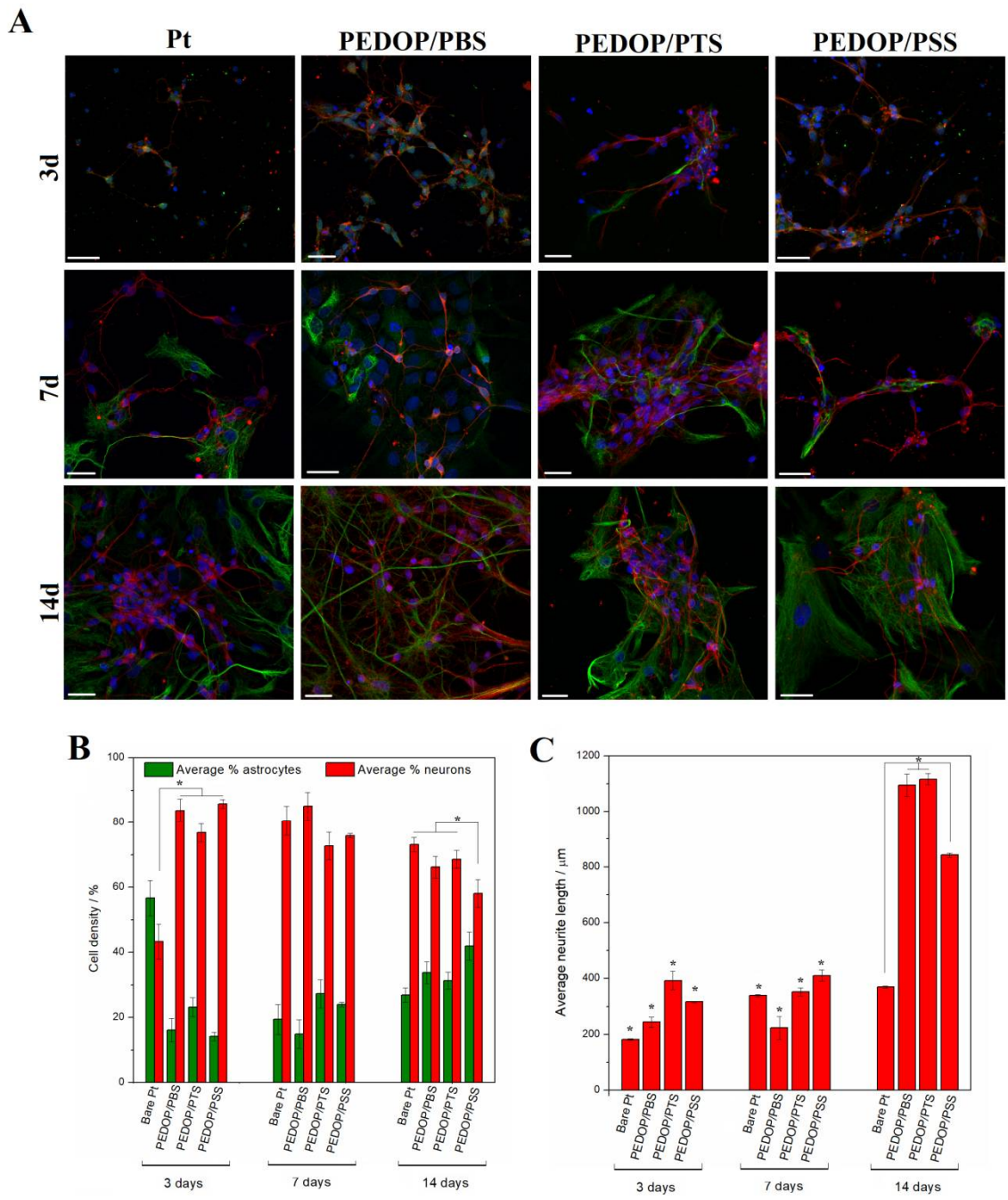

Fig.7. Fluorescent images of primary ventral mesencephalic (VM) mixed cell population cultured on PEDOP/PBS, PEDOP/PTS, PEDOP/PSS and Pt control substrates for 3, 7 and 14 days; neurons as visualized by anti-β III tubulin (red), astrocyte cells by anti-GFAP (green) and nuclei by DAPI (blue), scale bar = 20 µm (A); cell density (%) of astrocytes and neurons on CNT films and Pt control substrates (B); average neurite length, µm (C); results are ± STD, ★ = $p < 0.05$, N=3.

Tables

Tab.1. EIS parameters determined from the equivalent circuit model employing Randles circuit; R_1 is solution resistance, R_2 is charge transfer resistance, W is the Warburg coefficient, P and n are constant phase element parameters, C is the capacitance calculated from a depressed semicircle model (constant phase element in parallel with a resistor).

	PEDOP/PBS	**PEDOP/PTS**	**PEDOP/PSS**
R_1 / Ω	108 ± 2	183 ± 2	112 ± 3
R_2 / Ω	224 ± 7	2498 ± 371	722 ± 8
W / Ω $s^{-1/2}$	258 ± 10	1503 ± 297	747 ± 9
P · 10^5	9.7 ± 0.5	190 ± 10	4.3 ± 0.1
n	0.76 ± 0.03	0.89 ± 0.02	0.83 ± 0.01
C / mF cm^{-2}	0.10 ±0.01	8.13 ± 0.30	0.08 ± 0.01
χ^2· 10^4	7.09	3.03	0.85